Response to referee 2

We thank the anonymous referee for her/his comments. In the text below we respond point-by-point and discuss the changes to the work. The referee comments are written in black. Our answer to each comment is written below in blue. The proposed changes to the original manuscript are then highlighted in red.

General comments

This is strong manuscript that demonstrates impressive proficiency with many different sources of data (AWS, UAV, ICESat-2, modeling). The methods are generally well- described. The results section is very interesting and the development of spatially extensive aerodynamic roughness lengths for the K-Transect from ICESat-2 is commendable.

However, I do recommend some revisions. In its current form, the introduction is poor. Some of the terminology is vague, references are lacking and the overall research is poorly motivated. I encourage the authors to revise it thoroughly and have provided some ideas for doing so below.
We thank the reviewer for this feedback. We agree that the research could benefit by an improvement of the Introduction, and we have thus adapted parts of it and included more references. We hope that the updated introduction better motivates this study.

While it is useful to know that the commonly used method for deriving z0m from ICESat-2 (i.e. the standard deviation of ATL03 heights) tends to overestimate z0m, the new measure is slightly unsatisfactory if it underestimates z0m by a factor two. Without looking at the data, it is difficult to discern why. It could be due to the slightly arbitrary choice of filtering (qlow = 1 and qhigh = 2) to remove photons above and below the median. It could due to the choice gaussian covariance function, window size or assumed wavelength. Given that this is one of the first papers to investigate roughness lengths using ICESat-2 and availability of ground-truth data, it would be useful if the authors could develop a more unbiased method. I would encourage the authors to perform some sensitivity tests with these choices to see if they would reduce bias in their ICESat-2 z0m products.
We thank the reviewer for pointing out a very important issue that this study leaves unsolved : the systematic underestimation of z_{0m} when using the ICESat-2 measurements. Although we are also convinced that the current methods could be improved further, this would (given the current data) require an arbitrary tuning of the methods to fit the few available in situ observations. The arbitrary choices made in this study, such as the filter wavelength of 35 m, the median filter coefficients qlow = 1 and qhigh = 2, or the window size of 50 m, are unfortunately necessary in order to convert the raw photons to the final map of z_{0m}.

Nevertheless, we show that our results capture the observations well given the many uncertainties. Given that z_{0m} is often taken constant or used as a tuning parameter in atmospheric models, we consider them as very useful. Besides, our aim is to lay a foundation for more sophisticated studies. Furthermore, the high spatial variability of z_{0m} is a new result that has never been achieved using conventional in situ measurements. Finally, we would like to point out that z_{0m} ranges over nearly 4 orders of magnitudes over the Greenland Ice Sheet, and that it is the natural logarithm of z_{0m} that is used in atmospheric models to compute drag (our Eq. (1)). Therefore, we expect the 40% underestimation of z_{0m} that we have found in area A to have a limited impact on momentum drag and turbulent fluxes.

In order to give the interested reader the required information to improve our methods, we propose to add a sensitivity analysis in the Appendix.
In our new Fig. B1 we illustrate the impact of different filter wavelength Λ on the modelled z_{0m} at site S5. Our chosen value of 35 m gives the most acceptable results compared to the AWS observations.
In our new Fig. B2 we compare the interpolated elevation profiles from ICESat-2 ATL03 data using different covariance functions, different kriging radii different nearest neighbour ranges, and different median filter parameters, over two 200 m profiles in areas A and B. Changing these parameters does not lead to a clear improvement in elevation profiles.

Appendix B: Sensitivity experiments

Cutoff wavelength Λ

We find that the optimal value of the cutoff wavelength for the high-pass filter is $\Lambda = 35$ m. This may be explained by the fact that the resulting filtered topography using $\Lambda = 35$m still contains most (≈ 80 %) of the total variance of the slope spectrum. The latter is defined as the power spectral density of the first derivative of the elevation profile. A sensitivity experiment using different values for Λ at S5 can be found in Fig. B1. Changing the value for Λ strongly impacts the estimated H (Fig. B1c), as the elevation profiles considered here contain information at all wavelengths (Fig. B1a). On the other hand, increasing the value for Λ above 35m does not significantly affect the estimate frontal area index λ (Fig. B1b). Overall, increasing Λ from 10 m to 50 m increases the modelled z_{0m} from 7.6×10^4 m to 2.8×10^{-2} m at S5, in the direction 184° that matches the ICESat-2 track (Fig. B1d).

ATL03 kriging parameters

In order to interpolate the geolocated photons product ATL03 in a regular 1-m resolution elevation profile, a fixed set of interpolation parameters was used, referred to as the default set. These are the median filter coefficients in Eq. (7) $q_{low} = 1$ and $q_{high} = 2$, the median filter window length of 50 m, the choice of a gaussian covariance function with a radius of 15 m in the kriging equations,

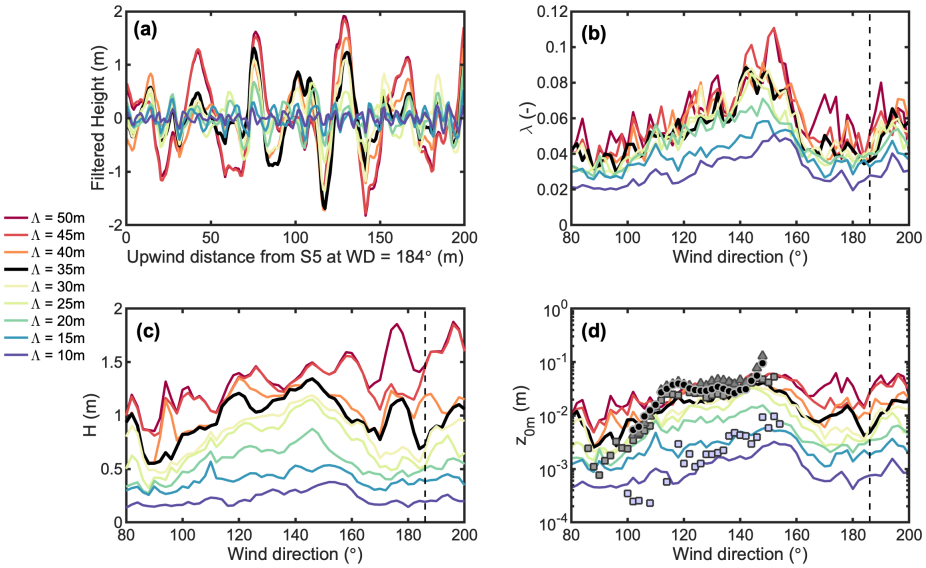

Figure B1: (a) Filtered elevation profile in direction 186°, (b) estimated obstacle frontal aera index, (c) estimated obstacle height and (d) modelled aerodynamic roughness length at site S5 for different high-pass cutoff wavelengths Λ. See Figure 8 in main text for the labels in d).

and the maximum distance of photon distance to each regular grid point of 15 m.

This default parameter set was found to give robust results, even when only medium or low confidence photons are present in the ATL03 data. A sensitivity experiment by varying each parameter separately in a 200-m portion of areas A and B is given in Fig. B2. While the interpolated ATL03 elevation still misses small-scale features present in the UAV data, varying each parameter does not give improved results (Fig. B2).

Specific comments

L16: Please consider capitalizing "ice sheet". It's the Amazon River, the Tibetan Plateau and should be the Greenland Ice Sheet. Indeed the Nature paper that you cite (Shepherd et al., 2020) has it this way.
The reviewer is correct. We have changed this accordingly, and we propose to use the acronym GrIS everywhere below L16, except in figure captions. The title of the manuscript was also corrected.
Title:
Mapping the aerodynamic roughness of the Greenland Ice Sheet surface using ICESat-2: Evaluation over the K-transect
L6:

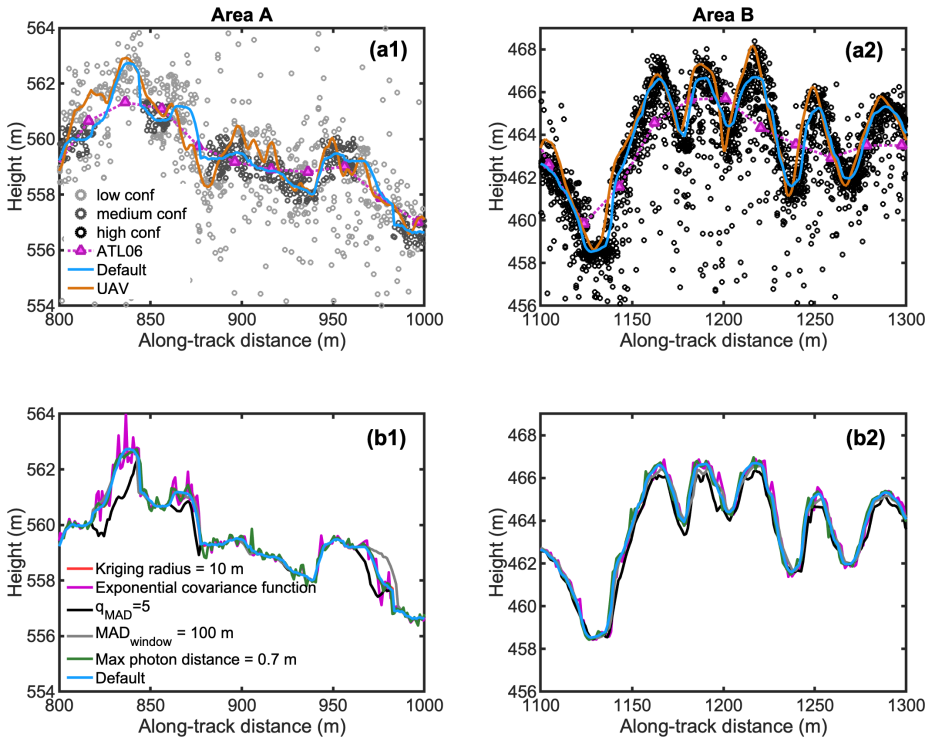

Figure B2: Elevation profiles in a 200-m portion of area A (left) and area B (right). The top panels contain the ATL03 data sorted in confidence levels (dots), the ATL06 data (pink triangles), the profiles measured by UAV photogrammetry (orange line) and the 1-m interpolated ATL03 data using the default settings used in the main text (blue line). The bottom panels contain the 1-m interpolated AT03 data using different origins and photon filtering settings.

We apply the model to a rough ice surface on the K-transect (western Greenland Ice Sheet) using UAV photogrammetry, (...)
L16:
Between 1992 and 2018, the mass loss of the Greenland Ice Sheet (GrIS) contributed (...)
L18:
Runoff occurs mostly in the low-lying ablation area of the GrIS, where (...)
L50: (...) profiles measured over the west GrIS by the ICESat-2 laser altimeter.
Figure 1:
(c) Location of the K-transect on the Greenland Ice Sheet.
L145:
(...) mass balance observations on the western part of the GrIS (...)
Figure 5:
(...) lower part of the K-transect, West Greenland Ice Sheet.

L351:
(...) spatio-temporal variability of the aerodynamic roughness length over the GrIS.
L19: If you define an acronym, it is usually appropriate to use it here and elsewhere (e.g. L50, L146).
We have replaced Greenland Ice Sheet by GrIS in the remainder of the manuscript (see reply above).

L18-21: Please provide some references for these two statements. A lot of work has been done on these topics and it is negligent to overlook it.
We agree with the reviewer. We propose to add the following references in this paragraph:

L18:
Runoff occurs mostly in the low-lying ablation area of the GrIS, where bare ice is exposed to on-average positive air temperatures throughout summer (e.g. Smeets et al, 2018; Fausto et al, 2021). As a consequence, the downward turbulent mixing of warmer air towards the bare ice, the sensible heat flux, is an important driver of GrIS mass loss next to radiative fluxes (Fausto et al, 2016 ; Kuipers Munneke et al, 2018; van Tiggelen et al, 2020).

Fausto RS, van As D, Box JE, et al (2016) Quantifying the surface energy fluxes in South Greenland during the 2012 high melt episodes using in-situ observations. Front Earth Sci 4:1–9. https://doi.org/10.3389/feart.2016.00082

Smeets PCJP, Kuipers Munneke P, van As D, et al (2018) The K-transect in west Greenland: automatic weather station data (1993–2016). Arctic, Antarct Alp Res 50:. https://doi.org/10.1080/15230430.2017.1420954

Kuipers Munneke P, Smeets CJPP, Reijmer CH, et al (2018) The K-transect on the western Greenland Ice Sheet: Surface energy balance (2003–2016). Arctic, Antarct Alp Res 50:S100003. https://doi.org/10.1080/15230430.2017.1420952

Fausto RS, van As D, Mankoff KD, et al (2021) PROMICE automatic weather station data. Earth Syst Sci Data Discuss 1–41. https://doi.org/https://doi.org/10.5194/essd-2021-80

Van Tiggelen M, Smeets PCJP, Reijmer CH, Van den Broeke MR (2020) A Vertical Propeller Eddy-Covariance Method and Its Application to Long-term Monitoring of Surface Turbulent Fluxes on the Greenland Ice Sheet. Boundary-Layer Meteorol. https://doi.org/10.1007/s10546-020-00536-7

L20: "can be" is poor rationale for studying something. Please revise with something stronger, perhaps relative to radiative heat fluxes.
We propose to modify this sentence (see our reply above).

L22-26: Again, please provide references to backup these statements. A paragraph in the introduction without any references indicates that the research is poorly motivated or that the authors have a complete lack of respect for previous research on this topic. Please revise.
We propose to add several references here to motivate this research further.
L22:
Although the strong vertical temperature gradient provides the required source of energy, it is the persistent katabatic winds that generate the turbulent mixing through wind shear (Forrer & Rotach, 1997; Heinemann 1999). Additionally, the surface of the GrIS close to the ice edge is very rough (Yi et al, 2005, Smeets & Van den Broeke, 2006). It is composed of closely spaced obstacles, such as ice hummocks, crevasses, melt streams and moulins. Due to the effect of form drag (or pressure drag), the magnitude of the turbulent fluxes increases with surface roughness (e.g. Garratt, 1992), thereby enhancing surface melt (Van den Broeke, 1996; Herzfeld et al, 2006). As of today, the effect of form drag on the sensible heat flux over the GrIS, and therefore its impact on surface runoff, remains poorly known.

Garratt, J. R.: The atmospheric boundary layer, Cambridge University Press, Cambridge, 1992.

Forrer J, Rotach MW (1997) On the turbulence structure in the stable boundary layer over the Greenland ice sheet. Boundary-Layer Meteorol 85:111–136. https://doi.org/10.1023/A:1000466827210

Yi, D., Zwally, H. J., and Sun, X.: ICESat measurement of Greenland ice sheet surface slope and roughness, Ann. Glaciol., 42, 83–89, https://doi.org/10.3189/172756405781812691, 2005.

Smeets, C. and Van den Broeke, M. R.: Temporal and spatial variations of the aerodynamic roughness length in the ablation zone of the greenland ice sheet, Boundary-Layer Meteorol., 128, 315–338, https://doi.org/10.1007/s10546-008-9291-0, 2008.

Herzfeld UC, Box JE, Steffen K, et al (2006) A Case Study or the Influence of Snow and Ice Surface Roughness on Melt Energy. Zeitschrift Gletscherkd Glazialgeol 39:1–42

Van den Broeke MR (1996) Characteristics of the lower ablation zone of the West Greenland ice sheet for energy-balance modelling. Ann Glaciol 23:7–13. https://doi.org/10.3189/s0260305500013392

L37: What do you mean by "confined accessible areas"? Please provide some examples.
We refer to areas that are accessible on glaciers for long-term in situ measure-

ments, so not the heavily crevassed areas or very remote areas. We propose the following clarification:
L37:
Historically, the surveying of rough ice was spatially limited to areas accessible for instrument deployment, possibly introducing a bias when it comes to quantifying the overall roughness of a glacier.

L39: Consider replacing "unmanned" with an ungendered term.
We agree with the referee and therefore propose to replace "unmanned areal vehicle" by "uncrewed aerial vehicle".
L39:
The recent development of airborne techniques, such as uncrewed aerial vehicle (UAV) photogrammetry and airborne LiDAR (...)

L40: What do you mean by "limited". Please be more specific.
We mean that airborne methods only cover portions of a glacier or ice sheet. We propose the following clarification:
40:
While these techniques enable the high resolution mapping of roughness obstacles, they often only cover portions of a glacier or ice sheet.

L41: I am not aware of a satellite altimeter that maps the surface roughness of entire glaciers. The ground sampling distance is not small enough. This sentence also makes it sound like UAVs are completely unnecessary. Please revise and be more specific.
Here we do not refer to roughness specifically, but to satellite remote sensing in general.
Concerning mapping the roughness: ICEsat data was used by Yi et al (2005) to map the roughness over the GrIS, and MISR data was used by Nolin & Mar (2019) to map the roughness of Arctic sea ice.
We propose the following clarification at L41.

Yi D, Zwally HJ, Sun X (2005) ICESat measurement of Greenland ice sheet surface slope and roughness. Ann Glaciol 42:83–89. https://doi.org/10.3189/172756405781812691
Nolin AW, Mar E (2019) Arctic sea ice surface roughness estimated from multi-angular reflectance satellite imagery. Remote Sens 11:1–12. https://doi.org/10.3390/rs11010050

L41:
On the other hand, satellite altimetry provides the means cover entire ice sheets, though the horizontal resolution remains a limiting factor when mapping all the obstacles that contribute to form drag.

L42-44: This sentence about sea ice does not fit here in a paragraph about glaciers and ice sheets, please move somewhere else.
Given the very few methods that were developed to map ice surface roughness using satellite data, we believe that mentioning these studies at this point in the

introduction is beneficial. Yet we propose the following modification to avoid further confusion:
L42:
Depending on the type of surface, parameterizations using available satellite products are possible, as presented for Arctic sea-ice by Lüpkes et al. (2013), Petty et al. (2017), and Nolin and Mar (2019).

L99-100: Presumably Fig. 1b could be referenced here?
Added
L99:
At this site, pyramidal ice hummocks with heights between 0.5 m to 1.5 m are superimposed on larger domes 100 of more than 50 m in diameter (see also Fig. 1b).

L145: missing an "of" between transect and AWS.
Added
L145:
"...140 km transect of AWS..."

L226: I thought you just said that this approach did not require interpolation to 1 m profile?
In Eq. (8) we use ATL03 raw photon data to calculate residual photon elevations. The approach that does not require 1-m interpolation is based on ATL06 data. We propose the following modification for clarification:
L224:
When working with the 1-m interpolated profile, we model the standard deviation of the unresolved topography (σ_{sub}) according to, ...

L252-259: This text would be more useful in the introduction.
We do also mention the issue of bulk model evaluations at L45-48 in the introduction.
L45:
The third and final challenge is the experimental validation of bulk drag models over remote rough ice areas, which either requires in situ eddy-covariance or multi-level wind and temperature measurements.

L260-274: Some more references to Fig. 6 in this paragraph would be useful to the reader.
We agree with the referee and therefore propose several additional reference to Fig. 6. We have also corrected "$\lambda < 0.05$" at line L270.
L260:
The L69 model (Eq.(A5)) overestimates z_{0m} for $\lambda < 0.04$ at this location (Fig. 6, blue line).
(...)
The method by M98 (Eq. (A6)) does account for the displacement height and, while using the same drag coefficient Cd = 0.25, it gives improved results for

$\lambda < 0.04$ (Fig. 6, green line) compared to L69. The same holds for the model by R92 (Fig. 6, red line).
(...) Using $C_d = 0.1$, all three models perform better for $\lambda < 0.04$ but perform poorly for $\lambda < 0.04$ (Fig. 6, dashed lines).

L285: Please clarify what is mean by "satellite backscatter". I presume you are referring to a satellite radar instrument since ICESat-2 does not measure backscatter.
We refer here to the broadening of a backscattered altimeter signals due to surface roughness. We propose the following modification:
L285:
Climate models and satellite altimeter corrections require information about the larger-scale spatial variability of surface (aerodynamic) roughness.

L288: Fig. 6? This figure does not show an elevation profile.
Corrected, we mean Fig. 5.
L288:
The elevation profile from the UAV survey in box A (Fig. 5) was already compared to the overlapping ICESat-2 profiles in Fig. 4a, while H, λ and z_{0m} are compared in Fig. 7.

Consider swapping Sections 4.1 to 4.2 and Fig. 5 and Fig. 6. I think it would make more logical to move from small to large scale.
We agree with the referee and thus propose to swap sections 4.1 and 4.2.

4 Results

4.1 Evaluation of the bulk drag model forced with a UAV DEM
(...)
4.2 Height of the roughness obstacles (H) estimated from ICESat-2
(...)
4.3 Evaluation of ICESat-2 roughness statistics against UAV DEMs

L396-397: It would be useful to briefly state again why Lettau (1969) is not recommended. Some people may only read the abstract and conclusions.
We agree and propose the following addition:
L396:
On the other hand, the use of the model of Lettau (1969) is not recommended over a rough ice surface, as it does not separate the form drag and the skin friction, and neglects both the effects of the displacement height and of inter-obstacle sheltering.

L399-402: I'm not sure I follow this logic. How do you know that ICESat-2 does not capture snow sastrugi or ice hummocks > 1000 m a.s.l. when your UAV surveys are constrained to <600 m a.s.l.?

As explained in L373-377, we have a crude estimate of these heights from field-work photographs. We propose the following addition for clarification:
L399:
Obstacles that are small compared to the ICESat-2 footprint diameter of ≈ 15 m, such as ice hummocks found above 1000 m elevation in summer, or snow sastrugi expected year-round at even higher locations on the ice sheet from photographic evidence, are not resolved by the ICESat-2 measurements when used in combination with the methods presented in this study.

L405: It's a bit of stretch to say ICESat-2 cannot map z0m above 1000 m when this study presents no UAV surveys above > 1000 m.
We hope that our study proves that ICESat-2 data can be used in the rough-ice areas below 1000-m elevation, given the uncertainties given in the reply above, and in the discussion. In order to convince the reader that the limitations above 1000 m are due to the ICESat-2 data and not to the bulk drag model, we have added a Figure in Appendix A and some explanatory sentences in the discussion:

L475:
Following the steps above, z_{0m} can be estimated for any H and λ, which is done in Fig. A1. At areas A, B and site S5, H and λ are estimated from the UAV surveys and from ICESat-2 data. At site S6, we assume that $H = 0.6 \pm 0.1$ m and $\lambda = 0.045 \pm 0.015$, based on photographs taken during the end of the ablation season. At the highest site S10, we assume that $H = 0.3 \pm 0.2$ m and $\lambda = 0.02 \pm 0.01$, which are typical values for sastrugi (Andreas, 1995).
L378:
Higher up, the ice hummocks become even smaller and the surface eventually becomes snow-covered year-round. Nevertheless, snow sastrugi, known to reach up to 0.5 m height at site S10 from photographic evidence, still contribute to form drag. This results in a maximum observed value of $z_{0m} = 7 \times 10^{-4}$ m at sites S9 and S10 (Fig. 10). Using a rough estimate for both H and λ at S6 and S10, based on photographs taken during the end of the ablation season, yields more realistic values for z_{0m} (Fig. A1) than using H and λ from the ICESat-2 elevation profiles. Therefore we conclude that the roughness obstacles are not properly resolved at these locations in the ATL03 data using the algorithm presented in this study, even when the correction using the residual photons scatter is applied.

Figure 1. Most of panel (a) is irrelevant, given that data from S9 are not used in this study. It makes it difficult to see how the ICESat-2 tracks intersect the UAV survey grids (A and B). Please consider removing the picture of S9 and providing a zoomed version of the UAV survey grids around the margins of the ice sheet. In the caption please specify if these are the ICESat-2 reference ground tracks or from an actual ICESat-2 beam (e.g. 1r).
We thank the referee for this suggestion. Yet we believe that a perspective

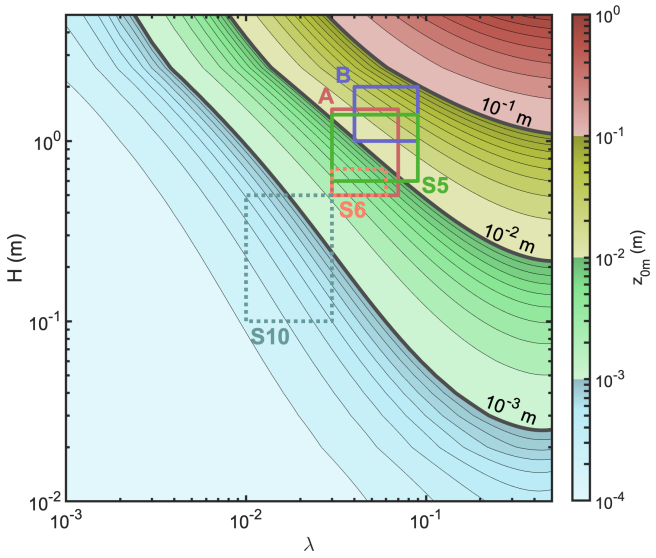

Figure A1: Estimated z_{0m} using the R92 model with parameterized C_d (Appendix A), as function of obstacle height H and frontal area index λ.The solid squares denote the estimated H and λ at three sites using UAV surveys. The dashed squares are first-order guesses based on photographs. See Fig. 1 for the location of each site.

over the whole K-transect is beneficial for the reader interested in the higher elevations. Especially given our reply to the above comment, Fig.1 is helpful to understand why ICESat-2 does not detect any obstacles above 1000 m elevation. Besides, we do show data from S6, S9 and S10 from both in situ measurements and ICESat-2 in Fig. 10.
We have added a reference to Table 2 in the text and in the caption of Fig.1 where the details about each ICESat-2 beam can be found:

L184:
A typical geolocated photon measurement ATL03 (Neumann et al., 2019) can be seen in Fig. 3 for site S5, and in Fig. 4a for area A. Details about which ICESat-2 measurements are compared against the UAV surveys are provided in Table 2.

Figure 2: What is the rationale for these wind directions? Prevailing wind direction from AWS? Please clarify.
These four wind direction are indeed prevailing wind direction, and were chosen to illustrate the variability of the surface topography.
L97:
Four measured elevation profiles, and a high-resolution orthomosaic image are

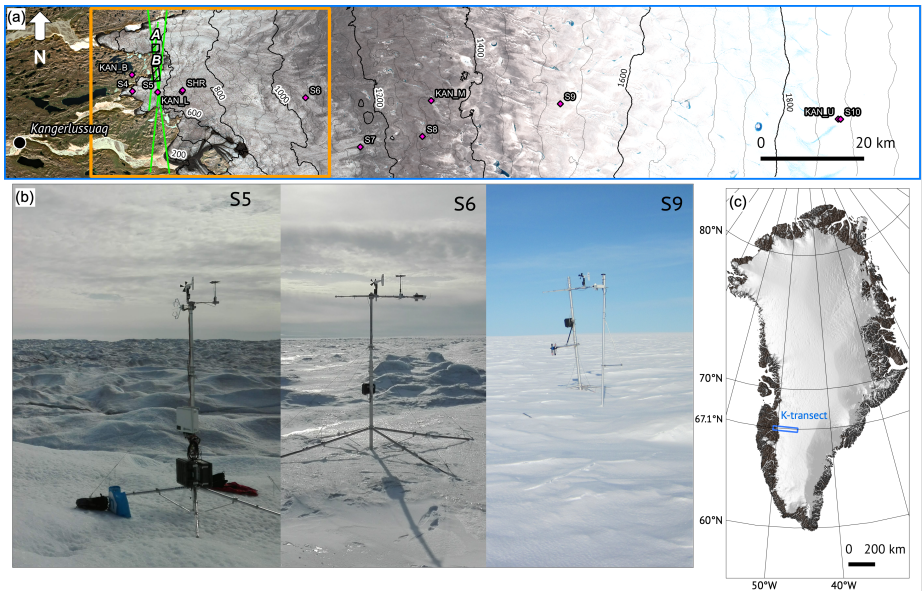

Figure 1: (a) Map of the K-transect, with the location of the automatic weather stations and mass balance sites indicated by the pink diamonds. The black boxes A and B delineate the areas mapped by UAV photogrammetry. The large black box indicates the area covered in Figs. 5 and 9. The background image was taken by the MSI instrument (ESA, Sentinel-2) on 12-08-2019. Pixel intensity is manually adjusted over the ice sheet for increased contrast. The green solid lines denote the ICESat-2 laser tracks that are compared to the UAV surveys (Table 2). (b) Sites S5 (06 Sep 2019), S6 (06 Sep 2019) and S9 (03 Sep 2019) taken during the yearly maintenance. Note that no data from the the AWS shown at S9 is used in this study. (c) Location of the K-transect on the Greenland ice sheet.

shown in Fig. 2. These were measured on 6 September 2019 at site S5 (67.094° N, 50.069° W, 560 m) in the locally prevailing wind directions, using UAV photogrammetry, of which the details will be given in Sect. 3

Figure 6: There is no reason for such large x and y axis limits on this figure which makes it difficult to determine the correspondence between the SEC and VPEC dots and modeled lines. Please provide a zoomed version of this figure. We agree with the referee and have reduced the extent of the x and y axis of Fig. 6. We also replaced "Observations" by "Estimated from in situ observations" after the feedback of referee #1.

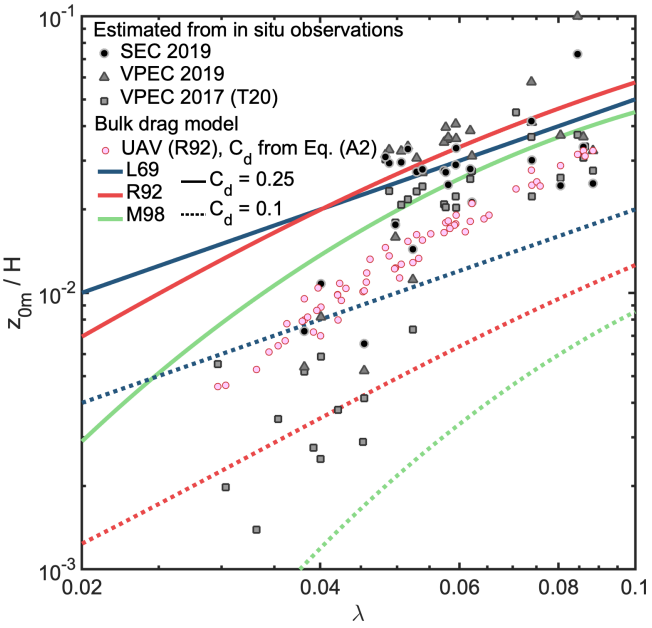

Figure 6: Modelled z_{0m} at site S5 using three different bulk drag models: Lettau (1969, L69, blue lines), Macdonald et al. (1998, M98, green lines), Raupach (1992, R92, red lines) and using two different values for the drag coefficient for form drag: $C_d = 0.25$ (solid lines) and $C_d = 0.1$ (dashed lines). Solid grey symbols are measurements from sonic eddy-covariance (SEC) or vertical propeller eddy-covariance (VPEC). Additional data are from Van Tiggelen et al. (2020, T20). Pink circles are the model results forced with H and λ from UAV photogrammetry, using the R92 model and C_d parameterized using Eq. (A2).